Host in Host Supramolecular Core-Shell Type Systems Based on Giant Ring-Shaped Polyoxometalates

Clement Falaise, Soumaya Khlifi, Pierre Bauduin, Philipp Schmid, William Shepard, Anton A Ivanov, Maxim N Sokolov, Michael A Shestopalov, Pavel A Abramov, Stéphane Cordier, et al.

Host in Host Supramolecular Core-Shell Type Systems Based on Giant Ring-Shaped Polyoxometalates

Clément Falaise,[a],* Soumaya Khlifi,[a] Pierre Bauduin,[b] Philipp Schmid,[b] William Shepard,[c] Anton A. Ivanov,[d] Maxim N. Sokolov,[d] Michael A. Shestopalov,[d] Pavel A. Abramov,[d], [e] Stéphane Cordier,[f] Jérôme Marrot,[a] Mohamed Haouas,[a] and Emmanuel Cadot [a],*

[a] Dr C. Falaise, Dr. S. Khlifi, Dr. J. Marrot,Dr. M. Haouas, Prof. E. Cadot
Institut Lavoisier de Versailles, CNRS, UVSQ, Université Paris-Saclay, Versailles, France
E-mail : clement.falaise@uvsq.fr & emmanuel.cadot@uvsq.fr
[b] Dr. P. Bauduin, P. Schmid,
ICSM, CEA, CNRS, ENSCM, Université Montpellier, 34199 Marcoule, France
[c] Dr. W. Shepard
Synchrotron SOLEIL, L'Orme des Merisiers, Saint-Aubain BP 48, 91192 Gif-sur-Yvette, CEDEX, France
[d] Dr. A. A. Ivanov, Prof. M. N. Sokolov, Dr. P. A. Abramov,
Nikolaev Institute of Inorganic Chemistry SB RAS, Novosibirsk, 630090, Russia
[e] Dr. P. A. Abramov
South Ural State University, Prospekt Lenina, 76, 454080, Chelyabinsk, Russia
[f] Dr. S. Cordier
Univ Rennes, CNRS, Institut des Sciences Chimiques de Rennes, ISCR – UMR 6226, F-35000 Rennes, France

Abstract: Herein, we show how the chaotropic effect is able to accelerate significantly supramolecular organizations during the acidification of aqueous solution of reduced molybdate ions. Time-resolved Small Angle X-ray Scattering (SAXS) analysis suggests that molybdenum-blue oligomeric species form huge aggregates in the presence of γ-cyclodextrin (γ-CD) which results in the fast formation of nanoscopic $\{Mo_{154}\}$-based host-guest species, while X-ray diffraction analysis reveals that the ending-point of these dynamic supramolecular organizations involving γ-CD results in an unprecedented well-ordered core-shell-like motif. A similar three-component core-shell like arrangement was found by using preformed hexarhenium chalcogenide-type cluster $[Re_6Te_8(CN)_6]^{4-}$ as exogenous guest. This seminal work brings better understanding of the self-assembly processes in general and gives new opportunities for practical applications in the design of complex multicomponent materials via the simplicity of the non-covalent chemistry.

Introduction

Self-assembled nano-objects combining organic and inorganic components represent an intense field of research.[1],[2] Important breakthroughs in this area have been reported leading to nanostructures efficient for energy conversion, storage or transport, drug delivery, gas capture or separation.[3],[4] As self-assembly is one of the most relevant approaches for the bottom-up construction of multifunctional materials, fundamental understanding of the molecular interactions is still critical for the rational design of specific supramolecular architectures.[5] Among contributing phenomena that include usual weak attractive forces such as coulombic, hydrogen bonding or dispersion forces, solvent effects are often underestimated, while they may contribute significantly to the stability of seemingly fragile supramolecular complexes. In context, unique solvation properties of water has been pinpointed out within numerous aggregation phenomena,[6],[7] and recent observations evidence the predominant role of water self-organization within supramolecular architectures associating ionic hydrophilic inorganic components and non-ionic molecules. For instance, host-guest assemblies involving dodecaborate anion $[B_{12}X_{12}]^{2-}$ (X = Cl, Br or I) or a cationic tantalum cluster $[Ta_6Br_{12}(H_2O)_6]^{2+}$ with γ-cyclodextrin have revealed exceptional high stability in water, even larger than those usually found with hydrophobic guests.[8],[9]
The pioneering works of Hofmeister in the end of the 19th century allowed discriminating two distinct behaviours of solvated ions regarding their effect on co-solutes, namely the salting-in of chaotropes and the salting-out of kosmotropes characterized respectively by a loosely and strongly bound hydration shell.[10],[11] Recent observations unveiling the remarkable supramolecular behaviour of low-charge density inorganic polynuclear ions expanded the Hofmeister series toward super-chaotropic species including polyoxometalates (abbreviated POMs) or boron clusters.[12],[13],[14],[15] POM compounds correspond to a wide structural class of discrete metal-oxo anionic species[16],[17] that encompasses unique electronic properties finding applications in many areas such as catalysis, biology or materials science.[18],[19] Nevertheless, in contrast to their growing interest, studies of the general behaviour of POMs in aqueous solution need much more attention, especially for their fine control and use at the supramolecular level. POMs are mostly considered as hydrophilic substances but they interact strongly with apolar cations such as alkyl ammonium ions to give extremely low solubility precipitates in water. This common behaviour, well-known by the POM chemists, concerns mostly the low-charge density POM species. Furthermore, hydrophobic effect has been found to contribute significantly to the plugging process of organic ions

at the surface of nanoporous polyoxometalate-based capsules, namely the Keplerate-type anions.[20] At the same time, other reports identified the chaotropic effect as the main contributor within self-assembly processes, such as host-guest recognition involving γ-cyclodextrin as non-ionic solute and dodecaborate anions[7] or POMs adsorption at the surface of non-ionic surfactant-based micelles.[21] Actually, the extremely high stability constants found for such hybrid organic-inorganic assemblies suggest that the (super)-chaotropic effect should be considered among the conglomerate of contributors as a generic driving force in supramolecular chemistry.[22] More recently, the chaotropic effect has been pinpointed out within the formation of POM-based globular assemblies or blackberry-like structures.[23],[24]

Here we report on the aqueous solution behaviour of the giant Mo-blue ring-shaped polyoxometalate $[Mo_{154}O_{462}H_{14}(H_2O)_{70}]^{14-}$ (abbreviated $\{Mo_{154}\}^{14-}$ and shown in Fig. 1a)[25],[26] in the presence of γ-cyclodextrin (noted γ-CD), a highly popular macrocycle for its remarkable hosting properties and related applications.[27],[28] Strikingly, when condensation of molybdates occurs under reducing conditions in the presence of γ-CD, a very fast growing process of $\{Mo_{154}\}^{14-}$ was detected by small-angle X-ray scattering (SAXS) analysis. Formation mechanism of the nanosized $\{Mo_{154}\}^{14-}$ species appears consistent with a pre-association step of molybdate-based oligomers around the γ-CD acting as a supramolecular template. Resulting species have been characterized structurally showing unprecedented nanosized core-shell type arrangement, reminiscent of the postulated host-guest template process. As proof of concept, this supramolecular host-guest template effect can even be deliberately reproduced using exogenous guests, such as chalcocyano hexarhenium cluster $[Re_6Te_8(CN)_6]^{4-}$, thus opening the way toward the design of hierarchical functional system. The superchaotropic character of the nanoscopic $\{Mo_{154}\}^{14-}$ ion is evidenced and has identified as the main contributor to the observed phenomena and behaviors in solution.

Results and Discussion

$\{Mo_{154}\}^{14-}$ in the Hofmeister series. We evaluated first the chaotropic behaviour of the $\{Mo_{154}\}^{14-}$ ion in aqueous solution using experimental procedure previously described by Buchecker et *al.* (Supplementary, section 1.3.1).[13] Such a method allows ordering ionic species as a function of their propensity to adsorb on non-ionic polyethylene glycol-based micelles. This was carried out by investigating the cloud point (CP) temperature of the C8E4 surfactant upon the addition of POMs, which refers to a liquid-liquid phase separation upon heating. The increase in the CP temperature upon addition of salts, *i.e.* salting-in effect has been found to depend on the adsorption strength of the ionic species at the surface of C8E4-based micelles.[31]

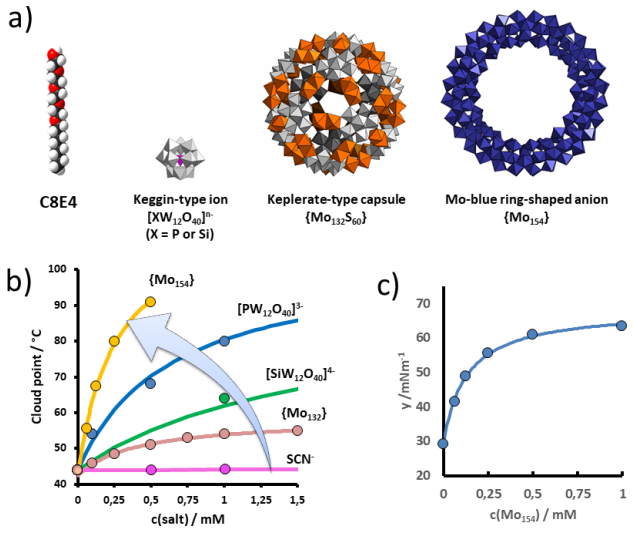

Figure 1. Including the superchaotropic Mo-blue ring shaped ion $\{Mo_{154}\}$ within the extented Hofmeister series: (a) Representation of the surfactant octyltetraethylene glycol $\{C_8H_{17}\text{-}(C_2H_4O)_4OH\}$ (noted C8E4) and archetypical polyoxometalates such as the Keggin type ion $[XW_{12}O_{40}]^{n-}$, the sulfurated Keplerate derivative $\{Mo_{132}S_{60}\}$ and the Mo-blue shaped ring $\{Mo_{154}\}$. (b) Variation of the cloud point (CP) of 60 mM C8E4 aqueous solution as a function of salt concentration showing the increasing of the chaotropic character along the thiocyanate-$\{Mo_{154}\}$ series. The solid lines represent the Langmuir isotherm fits that allow ordering these species within the Hofmeister series (see Supplementary section 1.3.2 for more details). (c) Surface tension (noted γ) of 60 mM C8E4 aqueous solution as a function of $\{Mo_{154}\}^{14-}$ concentration revealing the surfactant depletion from the water-air interface as the POM concentration increases.

Consequently, chaotrope species are identified and then classified according to their ability to increase the CP temperature of C8E4. As shown in Fig. 1b, addition of $\{Mo_{154}\}^{14-}$ increases markedly the CP temperature, showing

the strongest effect compared to i) other archetypical POMs i.e. the Keggin derivatives $[SiW_{12}O_{40}]^{4-}$ and $[PW_{12}O_{40}]^{3-}$ previously identified as super-chaotropes,[12] ii) the giant sulfurated Keplerate[32] $[Mo_{132}S_{60}O_{312}(H_2O)_{72}(AcO)_{30}]^{42-}$ ($\{Mo_{132}S_{60}\}^{42-}$) and iii) the classical SCN^- chaotrope. The Langmuir isotherm fitting reveals unambiguously that $\{Mo_{154}\}^{14-}$ exhibits the largest superchaotropic character in the series (Supplementary section 1.3.2). Furthermore, we studied variation of the surface tension of a 60 mM C8E4 aqueous solution as a function of $\{Mo_{154}\}^{14-}$ concentration (Fig. 1c and Supplementary section 1.3.3). The surface tension increase reflects the depletion of surfactant at the water-air interface, presumably because of significant association between the ring-shaped anion $\{Mo_{154}\}^{14-}$ and C8E4 occurring in the bulk of the solution. The origin of the extreme superchaotropic character of $\{Mo_{154}\}^{14-}$, compared to the other POMs should be understood on the basis of its large molecular surface supported by an extremely low charge density. Then, such a result anticipates unique supramolecular properties driven by this remarkable superchaotropic behavior.

Chaotropic effect from solution studies to structural model. Reports on the molecular growth of the Mo-blue ring-shaped anions suggest successive events corresponding to the linking of low nuclearity species, e.g. $\{Mo_8\}$, $\{Mo_2\}$ and $\{Mo_1\}$), identified as structural invariant units into high symmetry toroidal architectures, $[\{Mo_8\}_n\{Mo_2\}_n\{Mo_1\}_n]^{n-}$ with n = 14 or 16.[33],[34] Surely, the formation pathway from the starting to the ending-point is not straight-lined and must be marked out by a complex succession of efficient or non-efficient assays included within a set of converging or diverging events respectively in relationship with the cyclization process. The possible role of template effects has been hypothesized by Müller[35] and later unveiled by Cronin,[36],[37]using a flow reaction device enabling the isolation of a host-guest system resulting in a Krebs-type anion[36] $[Mo_{36}O_{112}(H_2O)_{16}]^{8-}$ encapsulated into a Mo-blue wheel. In this context, we reported previously that $\{Mo_{154}\}^{14-}$ anion was able to interact with γ-CD to give a non-classical "host in host" specieswherein the macrocyclic polysaccharide unit behaves as guest closely embedded within the large cavity of the inorganic torus.[38] Moreover, we also demonstrated that γ-CD was also able to interfere significantly in the condensation diagram of molybdate ions giving a striking $\{[Mo_6O_{19}]@(\gamma\text{-CD})\}^{2-}$ host-guest adduct.[39] In both cases, the (super)chaotropic nature of POMs was suggested as the key point, and could even decisively contribute to the self-aggregation and condensation processes as will be demonstrated here.

Herein, we investigate the influence of γ-CD upon kinetics of the $\{Mo_{154}\}^{14-}$ formation using time-resolved analytical tools such as SAXS, ^1H NMR and UV-vis (Supplementary, Section 1.2 for general methods). Time-resolved SAXS experiments have been carried out from 260 mM sodium molybdate synthetic solutions acidified at pH = 1 (see Supplementary Section 1.3.4 for full experimental details). As reported previously, the SAXS spectrum of colorless starting solution appears mostly dominated by the $[Mo_{36}O_{112}(H_2O)_{16}]^{8-}$ anion (Supplementary, section 2, Fig. S24).[26],[37],[40] Molecular growth leading to the $\{Mo_{154}\}^{14-}$ formation is initiated through addition of sodium dithionite as reducing agent, that results in an instantaneous color change from colorless to dark deep blue. In a first step, an abrupt increase of the scattering intensity is observed at $q < 0.1$ Å^{-1} from the first minutes following the addition of the reducing agent, while a second step is featured by a continuous increase of the scattering intensity within the low q values range ($q < 0.1$ Å^{-1}) until reaching a plateau after ~ 500 min. Furthermore, oscillations gradually shape at 0.21 and 0.42 Å^{-1} (see Fig. 2a) consistent with the increase in the $\{Mo_{154}\}^{14-}$ concentration (Fig. 2a and Supplementary section 1.3.4.2, Fig. S1-S3). At the first step corresponding to the first minutes after reduction, Guinier approximation analysis of the SAXS spectra is rather consistent with presence of entities larger than $[Mo_{36}O_{112}(H_2O)_{16}]^{8-}$ anion (Supplementary, section 1.3.4.3 and Fig. S6). This suggests that this first step should correspond to the fast formation of Mo-based oligomers under reducing conditions which convert slowly into the $\{Mo_{154}\}^{14-}$ species in a second step. In the presence of γ-CD (4 eq. per 154 Mo), SAXS spectra and related kinetic profile appear significantly altered, especially in the low q domain ($q < 0.02$ Å^{-1}) (Fig. 2b and Supplementary, section 1.3.4.2, Fig. S4). At the beginning of the process, the Mo-blue solution scatters strongly at lowq range while over the higher q domain, SAXS curves exhibit similar profiles to those observed in the absence of γ-CD (Supplementary, section 1.3.4.2, Fig. S4 and S5). This indicates that solution is still dominated by the presence of Mo-based oligomers but the strong scattering at low q ($q < 0.3$ Å^{-1}) suggests that they form very large supramolecular aggregates (larger than 300 nm!) in the presence of γ-CD. Surprisingly, these nano-aggregates disappear within less than 30 minutes for the benefit of species exhibiting a SAXS profile comparable to the one of the $\{Mo_{154}\}^{14-}$ anion (see Fig. S3). Interestingly, both events appear nicely correlated through a common kinetic process (Fig. 2c and 2d). Besides, scattering evolution exhibits an isosbestic point, meaning that complex mechanism of $\{Mo_{154}\}^{14-}$ formation from reduced Mo-based oligomers could be roughly simplified as a single step process, modelled fairly through a pseudo-first order kinetic (Fig. 2c, 2d and supplementary section 1.3.4.2).The presence of γ-CD increases significantly the rate constant up to 25 times ($\boldsymbol{k}_{obs}^{CD}/\boldsymbol{k}_{obs}$= 25), suggesting that γ-CD acts as a supramolecular catalyst favoring i) pre-concentration of the metal-oxo intermediates in the large aggregates around the γ-CD and ii) the cyclization process. The formation of very large aggregates take place immediately after the partial reduction of molybdates. We do not think that γ-CD could interfere with the basic mechanism of the $\{Mo_{154}\}^{14-}$ formation that encompasses elemental chemical steps corresponding to the making/breaking of Mo-O bonds, until the complete formation of the high symmetry Mo-torus. However, organic macrocycle should behave as a spool rolling up the Mo-based oligomers through supramolecular weak interactions as schematically depicted in Fig. 3. The formal mechanism must be intricate and the resulting analytical expression of $\boldsymbol{k}_{obs}$ constants should contain many terms reflecting these numerous elemental events.[33],[34] Nevertheless, as suggested by Müller, formation of the Mo-blue anions should result from connection

of few low nuclearity building blocks described as transferable units.[34] Then, this is the successive ordering transfer of these building blocks from the solution to the growing aggregates that generate the high symmetry assemblies. As written several years ago, a “hit-and-miss” type reaction scheme[41] could be postulated but taking into account the high degree of polymerization within the $\{Mo_{154}\}^{14-}$ macrocycle, an efficient discriminating routine must be integrated to reach the successful reaction path. In context, aqueous solvation modes of the Mo-based oligomers and related consequences upon the water-solute interfaces should be considered as a contributor within the self-assembly processes. Such species identified above as “superchaotropes” should exhibit hydration properties that have dramatic influence on all supramolecular processes, and thus affect the hydrogen-bonding network in the entire solvation shell. Chaotropic species have specific hydration thermodynamic fingerprints featured by high both enthalpy and entropy. This accounts for many physicochemical and/or supramolecular processes pinpointed by enthalpy-driven thermochemical process. Actually, the pathway leading to the formation of the ring-shaped anion $\{Mo_{154}\}^{14-}$ should range in such a scenario and could be dissected as a series of successive efficient events that minimize continuously the high energy water-solute interface. Fast dynamics, high flexibility and huge versatility that characterize the library of polyoxomolybdates in aqueous solution are certainly key points that make effective the directed growth toward molecular shape with the lowest surface/volume ratio. Additionally, it was also suggested that the sort of transferable bricks present in such aqueous solutions of molybdate ions dictates on their own the highly symmetrical $\{Mo_{154}\}^{14-}$ torus.[42] Such a statement holds only with the decisive contribution of the water molecules arising from the chaotropic nature of the POM precursors! Then, pre-aggregation process resulting from the interplay between γ-CD macrocycle and the dynamic library of molybdate-based building blocks should increase further probabilities of “hit” events that favor the cyclization process and then increase significantly the rate of the $\{Mo_{154}\}^{14-}$ formation.

Furthermore, using γ-CD as NMR probe, ^{1}H NMR study has been carried out to track the supramolecular interactions evolution along the $\{Mo_{154}\}$ formation process. Before introducing the reducing reagent, the ^{1}H NMR spectrum of 400 mM molybdate solution with a ratio γ-CD:Mo = 2:154 at pH = 1 is characteristic of the host-guest complex $\{[Mo_6O_{19}]@\gamma\text{-CD}\}^{2-}$ while in such conditions, the Krebs anion $[Mo_{36}O_{112}(H_2O)_{16}]^{8-}$ predominates (Supplementary, section 2, Fig. S14).[39],[43] Introducing the reducing reagent (sodium dithionite) provokes significant changes on the ^{1}H NMR spectrum which result mainly in the shielding of the H3, H5 and H6 hydrogen nuclei (Supplementary section 2, Fig. S15). It should be worth noting that the remaining H1, H2 and H4 resonances appear rather unaffected which preclude any paramagnetic effect on the chemical shifts. As the molybdate solution evolves toward the $\{Mo_{154}\}$ formation, the linewidth of the γ-CD resonances increases markedly from 10 to about 60 Hz, while the ^{1}H NMR chemical shifts appear quite unaffected (Supplementary, section 2, Fig. S15). Such an observation is consistent with conclusion drawn previously from the SAXS experiments. The formation of the large aggregates due to reducing conditions modifies noticeably the environment of the γ-CD as schematically shown in Fig. 3, but along the solution ageing, γ-CD is interacting permanently with the molybdenum-oxo oligomers, which are changing gradually from disordered, highly flexible and versatile into the highly ordered, rigid and structured $\{Mo_{154}\}^{14-}$ exoskeleton around the γ-CD. Such an evolution should not change in large extent the chemical shifts because the environment of the γ-CD remains quite similar, but must have strong consequences on the molecular dynamics, highlighted by the broadening of the resonances.

The crystallization process of the Mo-blue ring-shaped type anion in the presence of γ-CD has also been monitored by UV-vis spectroscopy in the visible-near infrared region (Supplementary section 1.3.7). The intensity changes with time of the two absorptions related to the Mo^{V}/Mo^{VI} intervalence charge transfer (IVCT) exhibit two distinct regimes. Below 60 min, increase of both IVCT absorptions appears nearly independent on the presence of γ-CD. This time domain should correspond to the structuring of the large mixed-valence Mo^{V}/Mo^{VI} oligomers. The second regime which becomes predominant above 60 min is identified by intensity decrease of both absorptions due to the deposition of crystalline solid which is accelerated drastically as the γ-CD content increases. Such an observation corresponds to a direct consequence of the increase of the $\{Mo_{154}\}^{14-}$ formation rate, previously evidenced by time-resolved SAXS experiments.

Finally, X-ray diffraction study of single-crystals grown from synthetic solutions containing 8 eq. of γ-CD per $\{Mo_{154}\}^{14-}$ unit (see Supplementary section 1.4 for synthetic procedures and section 1.3.6 for full structural details) revealed a similar striking hierarchical core-shell-like assembly which consists of the $\{Mo_{154}\}^{14-}$ torus as the first shell, hosting in its large cavity two superimposed supramolecular γ-CD-based guest units (Fig. 4). Interestingly, both guests themselves correspond to inclusion complexes wherein a Lindqvist-type anion $[Mo_6O_{19}]^{2-}$ appears closely embedded within the γ-CD cavity. It should be worth noting that these supramolecular inner host-guest arrangements are similar structurally to that previously reported and isolated from acidified molybdate solution under non-reducing conditions.[37] Nonetheless, the important lesson arising from the structural analysis of 1 lies in the presence of the γ-CD closely imbricated between inward and outward POM moieties, reminiscent of the Mo-based oligomers and γ-CD aggregates that drive the self-assembly process. Actually, this important feature underlines that solvent effects arising from the chaotropic nature of the POM species are strong enough to overcome the unfavorable electrostatic repulsions occurring between both outward and inward anionic units. These studies, included solution spectroscopies such as SAXS, NMR and UV-vis and X-ray diffraction analysis in the solid state demonstrate how intimate interplay between γ-CD and the dynamic library of molybdate-based

building blocks gives rise to efficient supramolecular templating effects leading to the formation of nanoscopic molecular core-shell-like species.

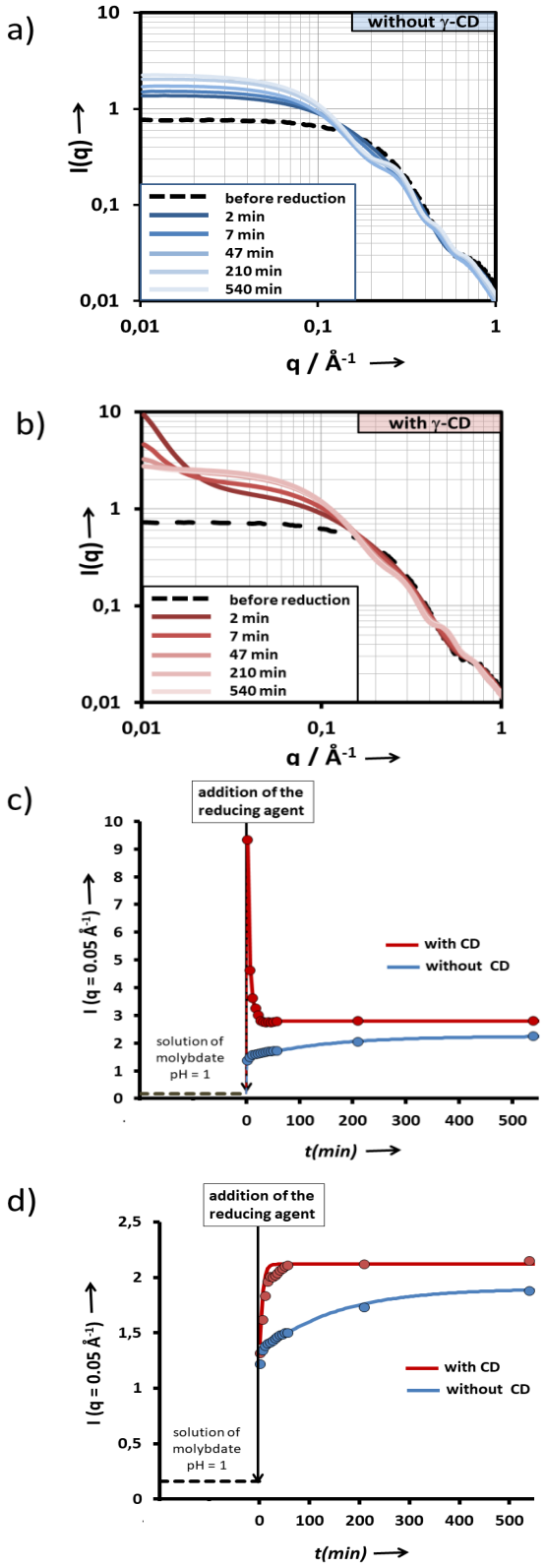

Figure 2. γ-CD influence on SAXS spectra and related kinetics of formation of the Mo-blue ring shaped $\{Mo_{154}\}^{14-}$ ion. Time-resolved SAXS curves (log(q)−log(I(q))) of Molybdenum-blue aqueous solutions in the (a) absence and (b) in the presence of γ-CD. Kinetic analysis of the time-resolved SAXS spectra carried out at (c) q = 0.01 Å^{-1} and (d) q = 0.05 Å^{-1}. Experimental data (circles) have been analyzed with a pseudo first-order kinetic regime (solid lines) highlighting the influence of the γ-CD by a 25-fold increase of the k_{obs} rate constant.

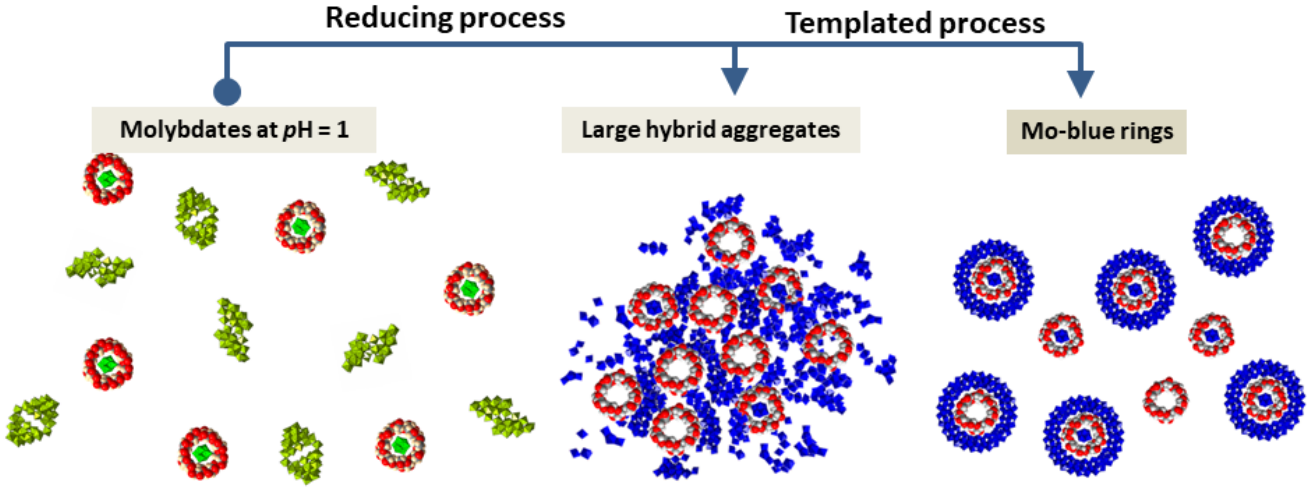

Figure 3. Schematic dissection of the $\{Mo_{154}\}^{14-}$ formation process into three main steps involving γ-CD as template (green polyhedron and blue polyhedron for oxidized and reduced Mo species forms, respectively). Before addition of the reducing agent (left), the starting aqueous solution of molybdates is mostly dominated by the presence of the Krebs anion $[Mo_{36}O_{112}(H_2O)_{16}]^{8-}$. Partial reduction of molybdate ions leads to Mo-containing oligomers (middle), presumably super-chaotropic entities forming very large hybrid aggregates with γ–CD that are rapidly converted into $\{Mo_{154}\}^{14-}$ hosting γ-CD (right).

Finally, X-ray diffraction study of single-crystals grown from synthetic solutions containing 8 eq. of γ-CD per $\{Mo_{154}\}^{14-}$ unit (see Supplementary section 1.4 for synthetic procedures and section 1.3.6 for full structural details) revealed a similar striking hierarchical core-shell-like assembly which consists of the $\{Mo_{154}\}^{14-}$ torus as the first shell, hosting in its large cavity two superimposed supramolecular γ-CD-based guest units (Fig. 4). Interestingly, both guests themselves correspond to inclusion complexes wherein a Lindqvist-type anion $[Mo_6O_{19}]^{2-}$ appears closely embedded within the γ-CD cavity. It should be worth noting that these supramolecular inner host-guest arrangements are similar structurally to that previously reported and isolated from acidified molybdate solution under non-reducing conditions.[37] Nonetheless, the important lesson arising from the structural analysis of 1 lies in the presence of the γ-CD closely imbricated between inward and outward POM moieties, reminiscent of the Mo-based oligomers and γ-CD aggregates that drive the self-assembly process. Actually, this important feature underlines that solvent effects arising from the chaotropic nature of the POM species are strong enough to overcome the unfavorable electrostatic repulsions occurring between both outward and inward anionic units. These studies, included solution spectroscopies such as SAXS, NMR and UV-vis and X-ray diffraction analysis in the solid state demonstrate how intimate interplay between γ-CD and the dynamic library of molybdate-based building blocks gives rise to efficient supramolecular templating effects leading to the formation of nanoscopic molecular core-shell-like species.

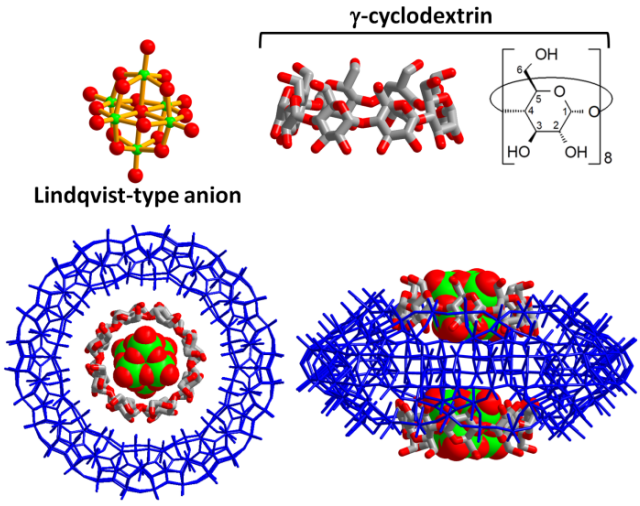

Figure 4. Mixed representation of supramolecular hierarchical assembly $[([Mo_6O_{19}]@(\gamma\text{-CD}))_2@[Mo_{154}O_{462}H_{14}(H_2O)_{70}]\}^{18-}$ found in 1a and 1b. (top) Highlight of the individual inner components consisting of the Lindqvist-type anion $[Mo_6O_{19}]^{2-}$ and γ-cyclodextrin. The organic macrocycle is composed of eight equivalent glucopyranose units. (bottom) Representation showing the deep inclusion of two Lindqvist-type anions $[Mo_6O_{19}]^{2-}$ themselves

embedded within γ-cyclodextrin hosts. The top-view highlights the perfect size and topology matching of the three components closely organized within a "Russian dolls-like assembly". The side-view reveals the two superimposed host-guest components $\{Mo_6O_{19}@\ \gamma\text{-CD}\}^{2-}$ plugging symmetrically the two apertures of the large $\{Mo_{154}\}^{14-}$ cavity.

Expanding the methodology with exogenous cluster as primary guest. These results open new opportunities for the design of hierarchical systems using the rich supramolecular chemistry that cyclodextrins offer. In this context, the octahedral-type cluster $[Re_6Te_8(CN)_6]^{4-}$ which interacts with γ-CD to form a highly stable 1:2 inclusion complex,[44],[45],[46] appears as an appropriate exogenous moiety for the large $\{Mo_{154}\}$-based container. From synthetic aqueous solutions containing the $[Re_6Te_8(CN)_6]^{4-}$ cluster, γ-CD and sodium molybdate in molar ratio 2:4:154 under reducing conditions at pH = 1, crystals of $Na_{24}\{([Re_6Te_8(CN)_6]@2(\gamma\text{-CD}))@[Mo_{152}O_{457}H_{14}(H_2O)_{68}]\}\cdot([Re_6Te_8(CN)_6]@2(\gamma\text{-CD}))\cdot 210H_2O$ (noted **2**) grew rapidly from aqueous solution allowing single-crystal X-ray diffraction analysis (see Supplementary, Sections 1.4 for synthetic procedure and 1.3.6 for structure refinement details). As shown in Fig. 5, the structure analysis reveals the large Mo- blue ring-shaped anion filled by the perfectly fitted host-guest complex $([Re_6Te_8(CN)_6]@2(\gamma\text{-CD}))^{4-}$, exemplifying nicely that such a methodology can be extended even to exogenous species that differ significantly in their nature (structure, electronic bonding and composition) from polyoxometalates. Interestingly, a non-centrosymmetric space group (C_2) was found in relation with the presence of a defect ring-shaped POM $\{Mo_{152}\}^{16-}$ which retains the C_1 trivial local symmetry instead of the high nominal D_{7d} symmetry related to the $\{Mo_{154}\}^{14-}$ ion.[47],[48] Consequently, the chiral components of the crystals, i.e. the two γ-cyclodextrins, have been fully located without any disorder or ambiguity. Otherwise, formation of this striking molecular core-shell-like arrangement cannot be explained from this resulting solid-state structure analysis which reveals only few short contacts and hydrogen bonds between the three components (see Supplementary, section 1.3.6.2 for full structural description of **2**). Then, this hierarchical assembly must be seen as the ending snapshot coming out from the context of intricate molecular recognition phenomenon occurring in solution, wherein the water molecules play a non-innocent and decisive contribution for strengthening the supramolecular interactions. In context, the chalcogenide-bridged $[Re_6Q_8(CN)_6]^{4-}$ clusters have been already classified as chaotropes owing to its host-guest thermochemical fingerprint.[44] Besides, X-ray diffraction analysis reveals an additional host-guest moiety located within a pocket surrounded by six $\{Mo_{152}\}^{16-}$ large tori (Supplementary, section 1.3.6.2, Fig. S12). As only few hydrogen bonding was found between few terminal oxygen atoms of the neighboring POMs and hydroxyl groups of the outer γ-CD, attractive electrostatic interactions involving Na^+ cations, which were not located through the successive structure refinements, should contribute obviously to the 3D packing.

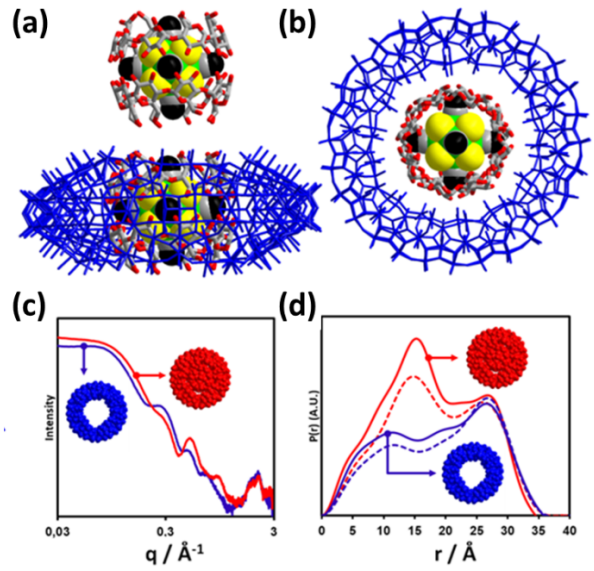

Figure 5. Structural representations and SAXS spectrum of supramolecular hierarchical assembly based on the hexa-rhenium type cluster, γ-CD and Mo-blue ring-shaped anion found in compound 2. (a) Representations of i) the deep inclusion of the rhenium-containing cluster into two γ-CDs forming the 1:2 supramolecular complex and ii) the 1:2 supramolecular complex inside the $\{Mo_{152}\}^{16-}$ exoskeleton highlighting the perfect fit between the nanoscopic host $\{Mo_{152}\}^{16-}$ and the $[Re_6Te_8(CN)_6]^{4-}$ cluster itself embedded within two γ-cyclodextrins (side-view). In such an arrangement, the central 1:2 inclusion complex $\{[Re_6Te_8(CN)_6]@2\gamma\text{-CD}\}^{4-}$ exhibits the same structural features as those previously reported for the isolated species (see ref. [44]). (b) Top-view of the core-shell like system showing the perfect host-guest complementarity between the three components. (c) SAXS spectra and (d), Pair distribution distance functions (PDDF) showing significant difference in scattering from inside the ring-shaped anion observed in the 15 ± 5 Å region (solid line = experimental, dotted line = calculated).

Such a mixed-metal core-shell-like assembly found in **2** yields specific SAXS features in aqueous solution resembling those of the template-free Mo-blue ring-shaped anion (Fig. 5c). Nevertheless, the Pair Distance Distribution Function (PDDF) deriving from the inverse Fourier transform of the scattering data exhibits distinctive

profile for a core-shell-like system (Fig. 5c-d and Supplementary section 1.3.5).[49] As shown in the PDDFs, the maximum linear extent for both species remains nearly identical and fits well with the crystallographic diameter of the torus Ø = 35-36 Å. Otherwise, the large guest-free torus gives rise to P(r) profile dominated by a bimodal electron density centered at about 11 and 26 Å consistent with the tire-type topology. As shown in Fig. 5d, the PDDF analysis undergoes characteristic changes with the molecular core-shell-like derivative related to the encapsulation of the heavy electron-scattering cluster that moves inward the region of high electronic density. This is nicely reflected by the appearance of a new intense peak centered at 15 Å due to a significant increase of the scattering probability from the interior part of the ring. Such a result agrees with frozen host-guest dynamics, mostly related to the solid-state arrangement and rather consistent with the ^{1}H NMR spectrum of **2** in aqueous solution (Supplementary, section 2, Fig. S19). It should be worth mentioning that such a scenario was not observed with the Lindqvist-containing $\{Mo_{154}\}^{14-}$ systems wherein SAXS and derived *P*(r) profiles remain nearly identical to those of the guest-free $\{Mo_{154}\}^{14-}$ torus (Supplementary, section 2, Fig. S24). Such a situation reflects a labile molecular core-shell system which involves mostly dissociative equilibria of the supramolecular assembly into individual molecular components in aqueous solution.

Conclusions

Understanding how the organic and inorganic assemblies interact at the nanoscopic scale is of utmost fundamental importance to the design of highly ordered hybrid systems. Here we demonstrate that the presence of γ-CD promotes aggregation of molybdate ions under reducing conditions. Solution studies supported by solid state analyses were consistent with mechanisms mostly directed by the chaotropic effect while this work demonstrates that the Mo-blue ring-shaped anion must be classified as the highest chaotrope in the Hofmeister extended series. Thus, such a property gives rise to important consequences corresponding to the significant increase of the formation rate of $\{Mo_{154}\}^{14-}$ or to the formation of related hierarchical multi-component architectures. SAXS studies suggested that γ-CD behaves as efficient supramolecular template forming very large hybrid aggregates rapidly digested into $\{Mo_{154}\}$-based systems. Besides, host-guest complementarity in size, topology and shape leads to striking molecular core-shell-like assembly incorporating exogenous species such as the electron-rich $[Re_6Te_8(CN)_6]^{4-}$ cluster. Such γ-CD templated process could be viewed as a molecular analogue of the liquid-crystal templated mechanism involved within the growth of the extended hexagonal honeycomb structure found in MCM-41.[50]

We imagine that such deliberate approach will provide new opportunities for tailoring multi-functional complex materials with spatial distribution of the individual complementary components, precise at the molecular level.

Acknowledgements

We acknowledge SOLEIL Synchrotron for providing beamtime and synchrotron radiation facilities on the SWING beam-line for the SAXS studies and the PROXIMA-2 for the single-crystal X-ray diffraction experiments and analysis. We especially thank Javier Perez for assistance in using swing beamline. The authors gratefully acknowledge IRP-CNRS CLUSPOM, CNRS MOMENTUM, and LabEx CHARMMMAT (Grant No. ANR-11-LBX-0039). This work was also supported by (i) University of Versailles Saint Quentin, (ii) CNRS, (iii) Region Ile de France through DIM Nano K. NIIC thanks the Ministry of Science and Education of the Russian Federation, and Embassy of France in Russia for the Vernadsky scholarship of A. A. I.

Keywords: supramolecular chemistry • inclusion compounds • cluster • polyoxometalate• cyclodextrin

[1] J. Dechnik, J. Gascon, C. J. Doonan, C. Janiak, C. J. Sumby, *Angew. Chem. Int. Ed.* **2017**, *56*, 9292–9310.
[2] G. O. Lloyd, J. W. Steed, *Nat. Chem.* **2009**, *1*, 437–442.
[3] M. Bonchio, Z. Syrgiannis, M. Burian, N. Marino, E. Pizzolato, K. Dirian, F. Rigodanza, G. A. Volpato, G. La Ganga, N. Demitri, S. Berardi, H. Amenitsch, D. M. Guldi, S. Caramori, C. A. Bignozzi, A. Sartorel, M. Prato, *Nat. Chem.* **2019**, *11*, 146–153.
[4] L. Ma, C. J. E. Haynes, A. B. Grommet, A. Walczak, C. C. Parkins, C. M. Doherty, L. Longley, A. Tron, A. R. Stefankiewicz, T. D. Bennett, J. R. Nitschke, *Nat. Chem.* **2020**, 1–6.
[5] M. S. Centellas, M. Piot, R. Salles, A. Proust, L. Tortech, D. Brouri, S. Hupin, B. Abécassis, D. Landy, C. Bo, G. Izzet, *Chem. Sci.* **2020**, DOI 10.1039/D0SC03243C.
[6] M. J. Langton, C. J. Serpell, P. D. Beer, *Angew. Chem. Int. Ed.* **2016**, *55*, 1974–1987.
[7] F. Biedermann, W. M. Nau, H.-J. Schneider, *Angew. Chem. Int. Ed.* **2014**, *53*, 11158–11171.
[8] K. I. Assaf, M. S. Ural, F. Pan, T. Georgiev, S. Simova, K. Rissanen, D. Gabel, W. M. Nau, *Angew. Chem. Int. Ed.* **2015**, *54*, 6852–6856.
[9] M. A. Moussawi, N. Leclerc-Laronze, S. Floquet, P. A. Abramov, M. N. Sokolov, S. Cordier, A. Ponchel, E. Monflier, H. Bricout, D. Landy, M. Haouas, J. Marrot, E. Cadot, *J. Am. Chem. Soc.* **2017**, *139*, 12793–12803.
[10] F. Hofmeister, *Naunyn-Schmiedelbregs Arch Pharmacol* **1888**, 247–260.
[11] W. Kunz, J. Henle, B. W. Ninham, *Curr. Opin. Colloid Interface Sci.* **2004**, *9*, 19–37.
[12] D. Kobayashi, H. Nakahara, O. Shibata, K. Unoura, H. Nabika, *J. Phys. Chem. C* **2017**, *121*, 12895–12902.
[13] T. Buchecker, P. Schmid, S. Renaudineau, O. Diat, A. Proust, A. Pfitzner, P. Bauduin, *Chem. Commun.* **2018**, *54*, 1833–1836.
[14] A. Solé-Daura, J. M. Poblet, J. J. Carbó, *Chem. – Eur. J.* **2020**, *26*, 5799–5809.
[15] M. Hohenschutz, I. Grillo, O. Diat, P. Bauduin, *Angew. Chem. Int. Ed.* **2020**, *59*, 8084–8088.
[16] M. T. Pope, *Heteropoly and Isopoly Oxometalates*, Springer-Verlag Berlin And Heidelberg, Berlin, Germany, **1983**.
[17] *Chem. Soc. Rev.* **2012**, *41*, 7325–7648.
[18] A. Misra, K. Kozma, C. Streb, M. Nyman, *Angew. Chem. Int. Ed.* **2020**, *59*, 596–612.
[19] I. A. Weinstock, R. E. Schreiber, R. Neumann, *Chem. Rev.* **2018**, *118*, 2680–2717.
[20] N. Watfa, D. Melgar, M. Haouas, F. Taulelle, A. Hijazi, D. Naoufal, J. B. Avalos, S. Floquet, C. Bo, E. Cadot, *J. Am. Chem. Soc.* **2015**, *137*, 5845–5851.

[21] B. Naskar, O. Diat, V. Nardello-Rataj, P. Bauduin, *J. Phys. Chem. C* **2015**, *119*, 20985–20992.
[22] K. I. Assaf, W. M. Nau, *Angew. Chem. Int. Ed.* **2018**, *57*, 13968–13981.
[23] Y.-F. Song, B. Qi, S. An, J. Lo, T. Liu, *Chem. – Eur. J.* **2020.**, *26*, 16802-16810.
[24] J. Chen, K. Qian, K. Xiao, J. Luo, H. Li, T. Ma, U. Kortz, M. Tsige, T. Liu, *Langmuir* **2020**, *36*, 10519–10527.
[25] A. Müller, E. Krickemeyer, J. Meyer, H. Bögge, F. Peters, W. Plass, E. Diemann, S. Dillinger, F. Nonnenbruch, M. Randerath, C. Menke, *Angew. Chem. Int. Ed. Engl.* **1995**, *34*, 2122–2124.
[26] A. Müller, S. K. Das, V. P. Fedin, E. Krickemeyer, C. Beugholt, H. Bögge, M. Schmidtmann, B. Hauptfleisch, *Z. Für Anorg. Allg. Chem.* **1999**, *625*, 1187–1192.
[27] D. Prochowicz, A. Kornowicz, J. Lewiński, *Chem. Rev.* **2017**, *117*, 13461–13501.
[28] S. Polarz, B. Smarsly, L. Bronstein, M. Antonietti, *Angew. Chem. Int. Ed.* **2001**, *40*, 4417–4421.
[29] B. Andersson, G. Olofsson, *J. Chem. Soc. Faraday Trans. 1 Phys. Chem. Condens. Phases* **1988**, *84*, 4087–4095.
[30] T. Buchecker, X. Le Goff, B. Naskar, A. Pfitzner, O. Diat, P. Bauduin, *Chem. – Eur. J.* **2017**, *23*, 8434–8442.
[31] Y. Zhang, S. Furyk, D. E. Bergbreiter, P. S. Cremer, *J. Am. Chem. Soc.* **2005**, *127*, 14505–14510.
[32] F. Bannani, S. Floquet, N. Leclerc-Laronze, M. Haouas, F. Taulelle, J. Marrot, P. Kögerler, E. Cadot, *J. Am. Chem. Soc.* **2012**, *134*, 19342–19345.
[33] H. N. Miras, C. Mathis, W. Xuan, D.-L. Long, R. Pow, L. Cronin, *Proc. Natl. Acad. Sci.* **2020**, *117*, 10699–10705.
[34] A. Müller, P. Gouzerh, *Chem. Soc. Rev.* **2012**, *41*, 7431–7463.
[35] A. Müller, P. Kögerler, C. Kuhlmann, *Chem. Commun.* **1999**, 1347–1358.
[36] H. N. Miras, G. J. T. Cooper, D.-L. Long, H. Bögge, A. Müller, C. Streb, L. Cronin, *Science* **2010**, *327*, 72–74.
[37] H. N. Miras, C. J. Richmond, D.-L. Long, L. Cronin, *J. Am. Chem. Soc.* **2012**, *134*, 3816–3824.
[38] M. A. Moussawi, M. Haouas, S. Floquet, W. E. Shepard, P. A. Abramov, M. N. Sokolov, V. P. Fedin, S. Cordier, A. Ponchel, E. Monflier, J. Marrot, E. Cadot, *J. Am. Chem. Soc.* **2017**, *139*, 14376–14379.
[39] C. Falaise, M. A. Moussawi, S. Floquet, P. A. Abramov, M. N. Sokolov, M. Haouas, E. Cadot, *J. Am. Chem. Soc.* **2018**, *140*, 11198–11201.
[40] T. Ito, T. Yamase, *Eur. J. Inorg. Chem.* **2009**, *2009*, 5205–5210.
[41] S. C. Lee, R. H. Holm, *Angew. Chem. Int. Ed. Engl.* **1990**, *29*, 840–856.
[42] A. Müller, C. Beugholt, *Nature* **1996**, *383*, 296–297.
[43] B. Krebs, S. Stiller, K. Tytko, J. Mehmke, *Eur. J. Solid State Inorg. Chem.* **1991**, *28*, 883–903.
[44] A. A. Ivanov, C. Falaise, P. A. Abramov, M. A. Shestopalov, K. Kirakci, K. Lang, M. A. Moussawi, M. N. Sokolov, N. G. Naumov, S. Floquet, D. Landy, M. Haouas, K. A. Brylev, Y. V. Mironov, Y. Molard, S. Cordier, E. Cadot, *Chem.- Eur. J.* **2018**, *24*, 13467–13478.
[45] A. A. Ivanov, C. Falaise, K. Laouer, F. Hache, P. Changenet, Y. V. Mironov, D. Landy, Y. Molard, S. Cordier, M. A. Shestopalov, M. Haouas, E. Cadot, *Inorg. Chem.* **2019**, *58*, 13184–13194.
[46] A. A. Ivanov, C. Falaise, D. Landy, M. Haouas, Y. V. Mironov, M. A. Shestopalov, E. Cadot, *Chem. Commun.* **2019**, *55*, 9951–9954.
[47] A. Muller, E. Krickemeyer, H. Bogge, M. Schmidtmann, C. Beugholt, S. K. Das, F. Peters, *Chem.- Eur. J.* **1999**, *5*, 1496–1502.
[48] S. Shishido, T. Ozeki, *J. Am. Chem. Soc.* **2008**, *130*, 10588–10595.
[49] M. Nyman, *Coord. Chem. Rev.* **2017**, *352*, 461–472.
[50] C. T. Kresge, M. E. Leonowicz, W. J. Roth, J. C. Vartuli, J. S. Beck, *Nature* **1992**, *359*, 710–712.